Microscope-Based Augmented Reality in Degenerative Spine Surgery: Initial Experience

Barbara Carl[1], Miriam Bopp[1,2], Benjamin Saß[1], Christopher Nimsky[1,2]

■ OBJECTIVE: **To establish microscope-based augmented reality (AR) support for degenerative spine surgery.**

■ METHODS: **Head-up displays of operating microscopes were used to establish AR in a series of 10 patients. Segmentation of the vertebra and additional target structures, which were visualized by AR, was based on preoperative magnetic resonance and computed tomography (CT) images, that were nonrigidly fused to low-dose intraoperative CT (iCT) data. AR registration was achieved by automatic registration applying iCT and microscope calibration.**

■ RESULTS: **AR support could be smoothly implemented in the surgical workflow. AR allowed to visualize the target structures reliably in the surgical field, facilitating surgical orientation. Flexible placement of the reference array enabled AR implementation for anterior, lateral, posterior median, and posterior paramedian approaches. Identification of bony and artificial landmarks allowed validating registration accuracy; the measured target registration error was 1.11 ± 0.42 mm (mean ± standard deviation). The effective dose for registration scanning ranged from 0.52 to 8.71 mSv, which is on average about one-third of a standard diagnostic spine scan. This depended mainly on the scan length (mean scan length cervical/thoracic/lumbar: 99/218/118 mm). Longest scan ranges were in the mid-thoracic region to ensure unambiguous vertebra assignment as prerequisite for reliable nonlinear registration (mean cervical/thoracic/lumbar effective dose: 0.52/6.14/2.99 mSv).**

■ CONCLUSIONS: **Reliable microscope-based AR support is possible because of automatic registration based on intraoperative imaging. Application of AR in degenerative spine surgery has a big potential; it might be especially helpful in complex anatomical situations and resident education.**

INTRODUCTION

Implementations of augmented reality (AR) environments are rapidly emerging in various fields covering commercial and consumer settings. Initially coming from military applications, it is now commonplace in aviation. There is a quickly emerging market for AR applications in health care. Cranial neurosurgery was 1 of the early adopters of AR technology in medicine. This was based on pioneering work in the 1980s with first attempts to integrate image injection systems in operating microscopes,[1,2] which led to commercial microscope-based implementations with integrated head-up displays (HUD) in combination with navigation systems in the mid-1990s.[3-7]

Despite microscope-based AR being used at different levels of sophistication for about 25 years in cranial neurosurgical procedures, spinal navigation setups have also been available for quite a long time, but only until very recently have experimental settings of implementations of AR for spine surgery been available and reported. Among these attempts to implement AR for spine procedures, there are reports of a percutaneous system for vertebroplasty[8] in cadaver studies for pedicle screw placements[9,10] and a feasibility study using AR for guidance in lumbar facet joint injections.[11] The microscope HUD was used for AR in a study to visualize osteotomy planes[12] and in a case study on cervical foraminotomy.[13]

Key words
- Augmented reality
- Head-up display
- Low-dose intraoperative computed tomography
- Microscope-based navigation
- Registration

Abbreviations and Acronyms
3-D: 3-Dimensional
AR: Augmented reality
CT: Computed tomography
ED: Effective dose
HUD: Head-up display
iCT: Intraoperative computed tomography
MRI: Magnetic resonance imaging
SD: Standard deviation
TRE: Target registration error

From the [1]Department of Neurosurgery, University Marburg, Marburg, Germany; and [2]Marburg Center for Mind, Brain and Behavior (MCMBB), Marburg, Germany

To whom correspondence should be addressed: Barbara Carl, M.D. [E-mail: carlb@med.uni-marburg.de]

Citation: World Neurosurg. (2019) 128:e541-e551.
https://doi.org/10.1016/j.wneu.2019.04.192

*Journal homepage: **www.journals.elsevier.com/world-neurosurgery***

*Available online: **www.sciencedirect.com***

1878-8750/$ - see front matter

We report on the implementation of microscope-based AR support for degenerative spine surgery applying a setting based on commercially available components.

MATERIALS AND METHODS

Ten patients (5 males, 5 females; age range: 38–84 years) underwent surgery for degenerative spine disease (Table 1) in a prospective case series. Patients were selected so that different kinds of approaches, positionings, and all spine sections were included. Informed consent was obtained from all individual participants included in the study. We obtained ethics approval for prospective archiving clinical and technical data applying intraoperative imaging and navigation (study no. 99/18).

In preoperative computed tomography (CT) and magnetic resonance imaging (MRI), the outline of the vertebral bodies was segmented automatically (anatomical mapping element, Brainlab, Munich, Germany), which was fine-tuned by additional manual segmentation. Segmentation was performed before surgery. Automatic vertebra segmentation needed about 2–5 minutes, depending on how many segments of the spine were included in the preoperative imaging. This automated segmentation result was inspected by the neurosurgeon performing the procedure and fine-tuned by manual adjustments, if necessary. Because the automatic segmentation result mainly depends on image quality of the preoperative images, the time needed for fine-tuning of the segmentation of the vertebra of interest was quite variable, with a range from 0 to 10 minutes. Additionally, depending on the pathology (e.g., the herniated disc or nerve roots), implants were segmented manually (smart brush element, Brainlab). All of these segmented objects were visualized by AR (Table 1).

The patient was placed in prone, lateral, or supine position on the x-ray lucent operating room table of a mobile 32-slice CT scanner (AIRO, Brainlab). Details of the surgical setting are published (Figure 1).[14] No patient movement was necessary during surgery. For scanning, the surgical area is covered with an additional sterile drape. Before skin incision, c-arm x-ray was used for level definition. In cervical procedures, the head was fixed with a head clamp. The reference array was attached to the head clamp in cervical procedures. In larger posterior approaches in the thoracic and lumbar spine, the reference array was attached to a spinous process, as in standard spinal navigation. In lateral approaches, it was attached to the retractor system used for the lateral approach while the patient was firmly immobilized. In all kinds of posterior approaches using only a minimal skin incision, it was firmly taped on the skin adjacent to the surgical approach.

Automatic AR registration was based on intraoperative CT (iCT). For registration scanning, a low-dose 70% protocol was used (helical acquisition, 120 kV, cervical: 28 mA, thoracic and lumbar: 33 mA). The navigation camera tracked the scanner during scanning for automatic registration of the CT images.[15] Registration scanning was done after performing the approach and placement of the retractor systems to avoid shifting of the structures. Registration accuracy was controlled by visualizing the pointer tip in relation to known structures, such as the retractor systems, as well as by fiducials placed on the skin close to the skin incision, which could be used for calculating the target registration error (TRE).

Table 1. Patient Characteristics, Diagnosis, Surgical Procedure, and AR Visualization

No.	Sex, Age	Diagnosis	Approach/Procedure	AR Visualization
1	M, 61	Recurrent lumbar disc herniation L3/4 right	Dorsal lumbar midline/removal of free disc segment spondylodesis L3/4	Vertebra L1–S5 and disc fragment
2	F, 73	Cervical myelopathy spinal stenosis C5/C6	Anterior cervical and posterior cervical/C5/C6 vertebral body replacement and C4-C7 lateral mass fixation	Vertebra C5 and C6
3	M, 60	Recurrent lumbar disc herniation L4/5 right	Dorsal lumbar midline/removal of free disc fragment and decompression	Vertebra L4–S5 and disc fragment
4	F, 38	Adjacent level disease after spondylodesis, pseudarthrosis L5/S1	Dorsal lumbar midline/L5/S1 cage revision and revision S1 screws, additional S2 screws	Vertebra L2–S5, cage L5/S1, posterior fixation (screws and rods)
5	M, 44	Lateral disc herniation L3/L4 right	Dorsal lumbar paramedian/removal of disc fragment	Vertebra C1–S5, disc L3/L4, disk fragment, nerve L3
6	F, 84	Lateral disc herniation L3/L4 left	Dorsal lumbar paramedian/removal of disc fragment	Vertebra L3 and L4, disc L3/L4, disk fragment, nerve L3
7	M, 50	Medial disc herniation T8/9	Lateral thoracic/removal of calcified disc herniation and posterior fixation T8/T9	Vertebra C1–S5, spinal canal, disk fragment
8	F, 67	Lateral disc herniation L4/L5 left	Dorsal lumbar paramedian/removal of disc fragment	Vertebra L4 and L5, disk fragment, nerve L4
9	F, 62	Medial disc herniation T8/9	Lateral thoracic/removal of disc herniation	Vertebra T8 and T9, disk fragment
10	M, 62	Foraminal stenosis L4/L5 left	Dorsal lumbar midline/decompression of L4	Vertebra L4 and L5, nerve L4

3-D, 3-dimensional; AR, augmented reality; CT, computed tomography; ED, effective dose; HMD, head-mounted device; HUD, head-up display; iCT, intraoperative computed tomography; MRI, magnetic resonance imaging; OR, operating room; SD, standard deviation; TRE, target registration error.

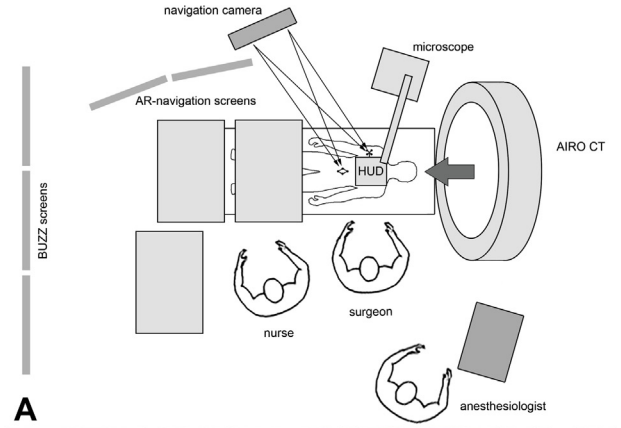

Figure 1. Overview of the operating room setting. (**A**) Schematic overview. (**B**) Actual intraoperative scene. *Black arrow* depicts how the navigation camera tracks the reference array and the microscope. AR, augmented reality; CT, computed tomography.

The effective dose was calculated by multiplying the dose length product referring to a phantom with a diameter of 16 cm in cervical and 32 cm for thoracic and lumbar examinations with conversion factors (cervical: 5.4 μSv/Gy*cm; thoracic: 17.8 μSv/Gy*cm; and lumbar: 19.8 μSv/Gy*cm).[16,17]

After a rough rigid prealignment, nonlinear registration of iCT data and preoperative image sets was performed (spine curvature correction element, Brainlab). Image fusion accuracy was carefully checked inspecting the close matching of the outline of the preoperatively segmented vertebra in the iCT images.

The HUD of the operating microscopes Pentero and Pentero 900 (Zeiss, Oberkochen, Germany) were used for AR visualization controlled by the microscope element application (Brainlab). Calibration of the HUD was performed by adjusting the superimposition of the 3-dimensional (3-D) representation of the reference array and the real structure of the reference array. After this step, AR registration accuracy was repeatedly ensured by focusing with the operating microscope on known structures like edges of the retractor systems, as well as on the attached skin fiducials and checking the position of the crosshair representation of the focus point in the AR visualization.

The microscope application allowed different modes of operation of the AR display. For AR, the segmented objects could be visualized in a semitransparent 3-D rendering or as dotted outlines in the microscope view. Individual colors could be assigned to the different objects, as well as each object could be switched off individually to avoid an information overflow, when an unobscured view of the surgical field was necessary. Additionally, on screens close to the surgical field various additional visualizations were available ranging from solid objects, additional semitransparent video overlay, in case the HUD was switched off, as well as different views of the image datasets in inline view, probe's eye view, as well as a 3-D overview visualizing how the video frame is related to the rendered 3-D AR objects and 3-D image sets of the whole scene.

RESULTS

In all 10 patients, AR support could be established reliably. The additional intraoperative time needed for iCT scanning and automatic AR registration was on average less than 5 minutes, including all surgical preparation steps (placement of registration array and draping: 2 minutes; CT scan: less than 10 seconds; removal of draping and accuracy documentation: 2 minutes), until full AR support was available.

The scan length of the iCT scan for AR registration ranged from 81 to 248 mm (mean ± standard deviation [SD]: 136 ± 55 mm). To achieve a reliable nonlinear registration between preoperative images and iCT images, especially in the mid-thoracic region, longer scan ranges were necessary to avoid false registrations from missing clear anatomical landmarks and to ensure unambiguous vertebra assignment as prerequisite for the nonlinear registration (mean scan length: cervical: 99 mm; thoracic: 218 mm; lumbar: 118 mm). This directly influenced the overall effective dose (ED) which ranged from 0.52 to 8.71 mSv (mean ± SD: 3.38 ± 2.22 mSv) (mean cervical ED, 0.52 mSv; mean thoracic ED, 6.14 mSv; mean lumbar ED, 2.99 mSv). Nonlinear registration accuracy could be checked by observing the matching of the 3-D representation of vertebra, which were segmented in the preoperative images, with the actual outline of the vertebral bodies in the iCT images. In the area of interest (i.e., the level of surgery), the deviation was in the range of 1 mm.

The measured TRE ranged from 0.57 to 1.59 mm (mean ± SD: 1.11 ± 0.42 mm). Additional landmark checks (e.g., identifying typical anatomical landmarks, such as the outline of the vertebral bodies, spinous process, or lamina; the edge of retractor structures; reflective balls) of the reference array allowed us to ensure high accuracy (**Figure 2**). Adjusting the AR outline of the reference array with the real structure at the beginning of AR usage in each case, allowed us to verify adequate AR microscope calibration (**Figure 3**). Repeated checking of the position of bony and artificial landmarks ensured ongoing registration accuracy during the course of surgery, verifying that the relation of the reference array to the actual surgical site was stable, excluding an unwanted movement of the reference array or a change in the relative vertebral body alignment.

Multiple objects, distinguishable by color, could be visualized applying AR (**Table 1**). The ability to switch off individual objects allowed to maintain a clear overview of the surgical field in case

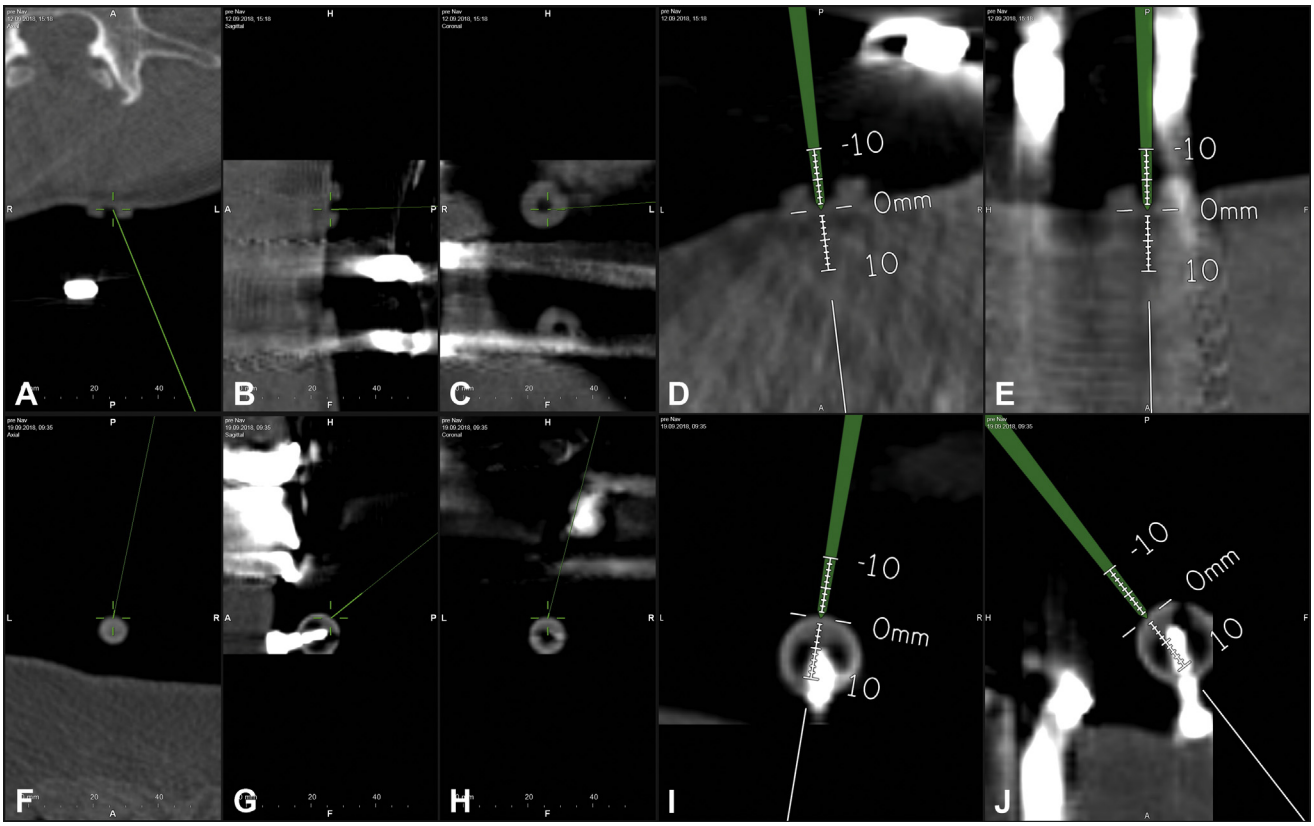

Figure 2. Documentation of registration accuracy. Placement of skin fiducials allows measurement and calculation of the target registration error from their known geometry, the pointer tip is placed in the middle of the fiducial. (**A**) Axial. (**B**) Sagittal. (**C**) Coronal. (**D-E**) Inline. Identification of the reflecting balls of the reference array with the navigation pointer allows additional documentation of ongoing correct patient registration. (**F**) Axial. (**G**) Sagittal. (**H**) Coronal. (**I/J**) Inline (the inline views show a millimeter scale at the pointer tip visualization).

too much AR information interfered with the clear overview and potentially irritated the surgeon. AR visualization applying the microscope HUD was used most of the time; the number of visualized objects was often reduced to the target object after having performed the major preparation steps, so that the display of the vertebra bodies was switched off. The ability to toggle the HUD on and off provided an unobscured surgical view if suddenly requested. The visualization of the AR video overlay on screens close to the surgical field provided continuous uninterrupted AR visualization, which is also available for all other surgical team members.

Smooth hand-eye coordination could be maintained at all surgical steps during usage of AR, because the 3-D AR visualization provided a good depth perception. This depth perception was supported by an additional separate visualization of how the microscope-viewing plane (i.e., the video frame) is placed in relation to a 3-D reconstruction of various image datasets and visualized objects. In parallel, standard navigation views in inline and probe's-eye views facilitated orientation. If necessary, the location of a pointer parallel to the use of the operating microscope could be visualized, allowing measurements in the surgical field, as well as providing further information on the viewing angle of the microscope (Figure 8C, D, G, H).

AR could be successfully used independent of the spine region and independent of the approach. The accuracy was not influenced by these parameters; however, a careful adjustment and stable placement of the reference array was mandatory to avoid a dislocation of the array during surgery. Because iCT scanning for AR registration was performed after approaching the spine and after placement of retractors, a positional shifting of the coordinate reference system was prevented.

AR could be applied in surgery for cervical stenosis and allowed to reliably visualize the outline of the vertebra during an anterior approach, facilitating their removal and speeding up surgery (Figure 4). In thoracic disc surgery, with a lateral approach, the visualized AR outline of the vertebra bodies eased orientation and allowed us to perform minimal bone drilling to access the median disc bulging (Figures 5 and 6). In lumbar midline approaches, AR facilitated the orientation in scar tissue during surgery of recurrent discs; it also allowed us to identify the position and removal of a cage in a patient undergoing revision surgery for pseudarthrosis (Figure 7). There was a close matching of the 3-D representation of the cage and its position in reality; inserted pedicle screws allowed further checking of AR visualization accuracy. The same close matching was observed in the case of the AR representation of a compressed nerve root in

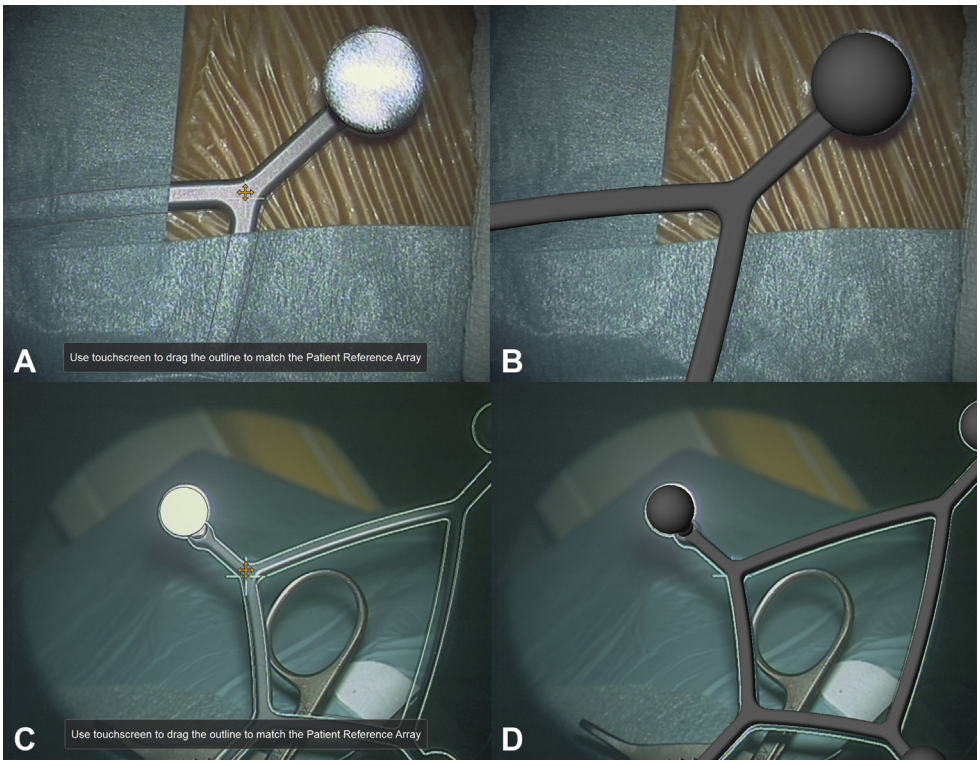

Figure 3. Augmented reality calibration check by visualization of the outline of the reference array applying the head-up display of the microscope as (**A**, **C**) a line representation or as (**B/D**) a 3-dimensional representation (in line representation mode an adjustment is possible). (**A/B**) Reference array firmly taped to the skin; (**C/D**) reference array attached to a spinous process with a clamp.

foraminal stenosis. In lumbar paramedian approaches for lateral disc surgery, AR clearly improved surgical orientation and allowed us to locate the nerve root and disc fragment (Figure 8).

DISCUSSION

Applying the HUD being integrated in the operating microscope, AR support for degenerative spine surgery could be successfully implemented based on commercially available system components for the first time. The principal concept had been demonstrated previously in 2 case reports in which the microscope HUD was used to visualize osteotomy planes[12] and applied for cervical foraminotomy.[13] As an alternative to the microscope, HUD for AR implementing head-mounted devices were investigated for their use in spine surgery, especially for percutaneous procedures such as kyphoplasty,[8,18] facet joint injections,[11] biopsies, and placement of pedicle screws.[9,10,19] However, in most of these concept studies the suggested registration setup cannot be actually transferred to the real clinical surgical situation because it needed some visual adjustment of reality and AR display. In our setting, low-dose iCT registration scanning allowed a user-independent straightforward and reliable registration process.

AR greatly supported anatomical orientation in all cases. Target structures such as herniated disc fragments could be localized quickly, which proved to be especially helpful in reoperations, in lateral thoracic approaches for median disc herniations, and in paramedian lumbar approaches for lateral disc herniations.

The advanced AR visualization in combination with additional views on screens near the surgical field provided a good 3-D perception, including good depth perception resulting in smooth hand-eye coordination, which is crucial when using such a technology.[20]

If AR is used during surgery not only for displaying images besides the surgical field, but actually for visualizing objects in the surgical field itself, a close matching of the visualized objects to reality such as correct registration is essential. Overall AR accuracy depends on several factors: 1) correct nonlinear image registration, which could be reliably checked by controlling the close matching of the segmented vertebra outlines; 2) correct calibration of the AR visualization device, such as in our study the HUD of the operating microscope, which could be checked by observing the overlay of the visualized registration array and reality, and most critical; and 3) correct patient registration.

User-independent patient registration, as can be established by intraoperative imaging, ensures high navigational accuracy, which was demonstrated for cranial procedures with a mean TRE of 0.93 mm.[15] In a study about augmented reality for transsphenoidal surgery, a significant benefit of automatic registration in comparison to fiducial-based registration with an improved mean TRE of 0.83 mm versus 2.33 mm was demonstrated.[21] These

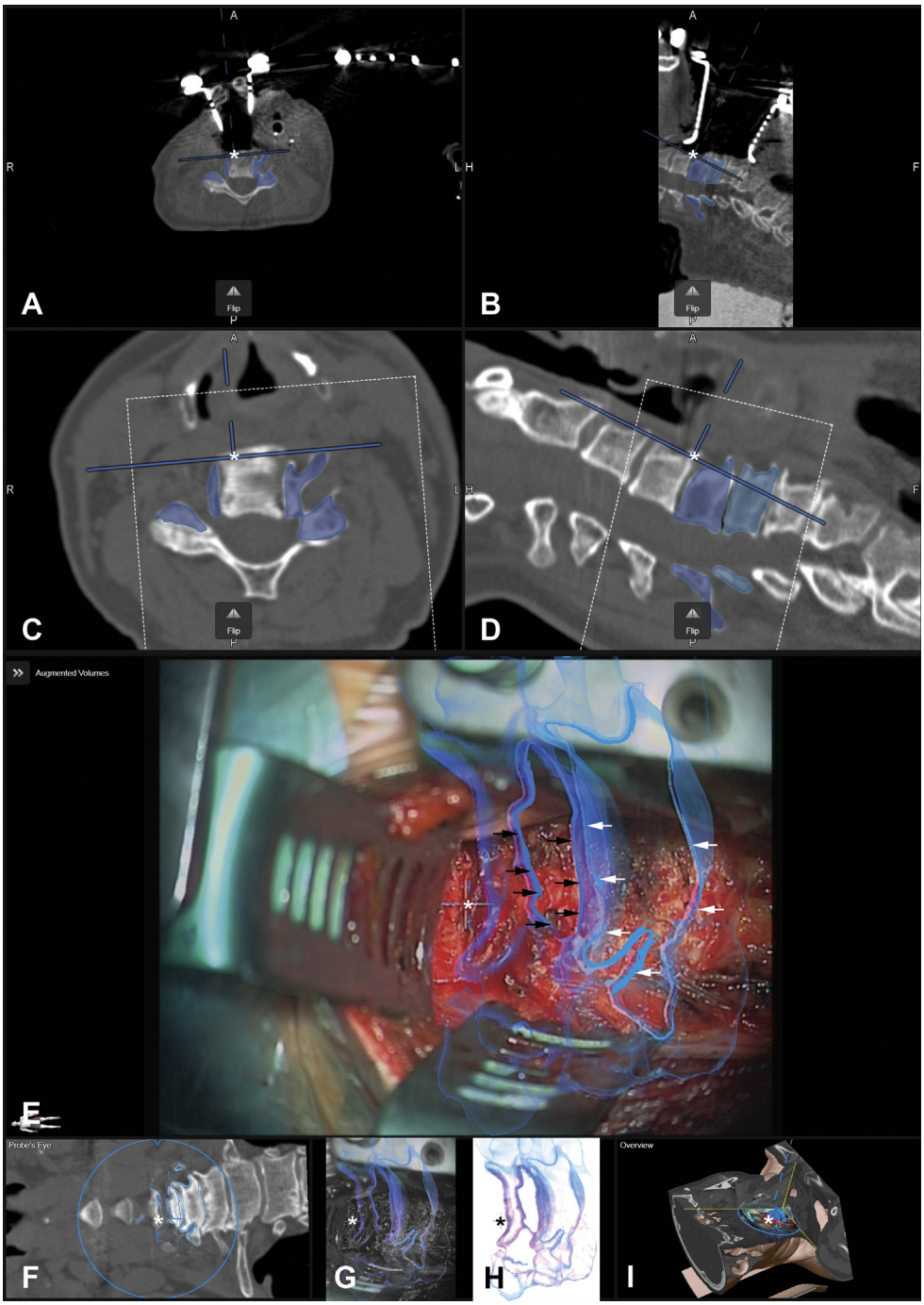

Figure 4. A 73-year-old female patient (case 2) with cervical myelopathy undergoing vertebral body replacement of C5 and C6 via an anterior approach. Intraoperative computed tomography (CT) images used for augmented reality (AR) registration, showing the viewing axis of the operating microscope: (**A**) axial, (**B**) sagittal view. Nonlinearly registered preoperative CT; the dotted white box marks the region of interest used for the nonlinear image registration: (**C**) axial, (**D**) sagittal view. (**E**) AR visualization of the outline of the vertebral bodies C5 and C6 in different tones of *blue*; the crosshair in the image center corresponds to the position of the microscope focus point, which is marked by an *asterisk* in all views; the *black arrows* depict the AR outline of C5 in the focus plane visualized thicker than the structures beyond the focus plane; the *white arrows* delineate the C6 outline in the focus plane. (**F**) The probe's-eye view of the preoperative CT images. (**G**) AR visualization over a grayed video frame. (**H**) AR visualization with a white background. (**I**) Overview depicting how the video frame is aligned to the 3-dimensional image data.

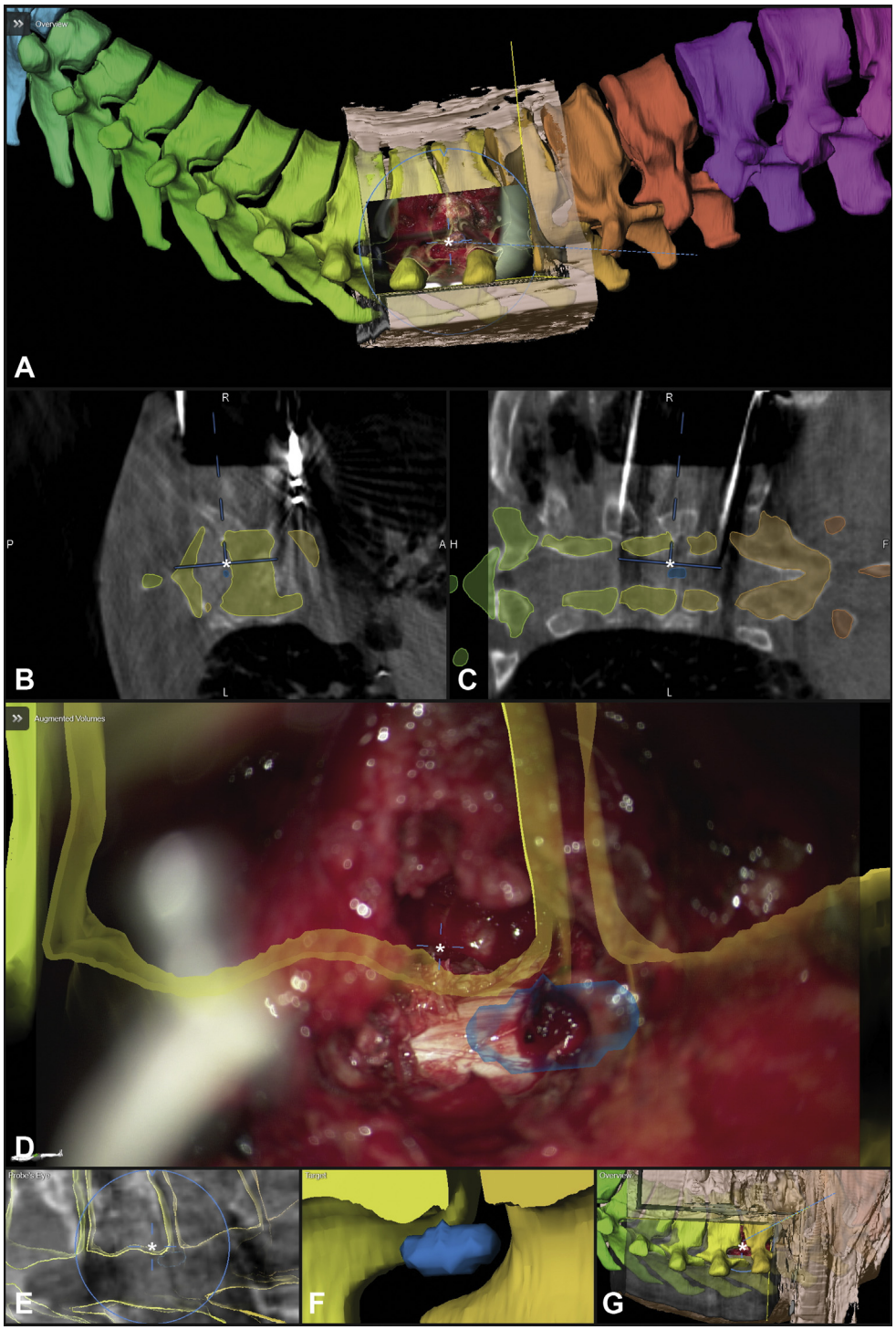

Figure 5. A 50-year-old male patient (case 7) with a medial disc herniation T8/9 removed via a lateral thoracic approach. (**A**) Overview visualization depicting the position of the microscope view in relation to the segmented vertebra which are visualized in 3-dimensional in individual colors. (**B**) Axial. (**C**) Coronal view of navigation screen of iCT images with the segmented vertebra, as well as the disc herniation (*blue*). (**D**) AR visualization with the outline of the vertebra bodies T7, T8, and T9 in different tones of *yellow* and *orange*. The dura is visible close to the segmented disc herniation (*blue outline*), the *blue crosshair* in the image center corresponds to the position of the microscope focus point which is marked by an *asterisk* in all views. (**E**) Probe's-eye view, (**F**) target view, (**G**) enlarged overview.

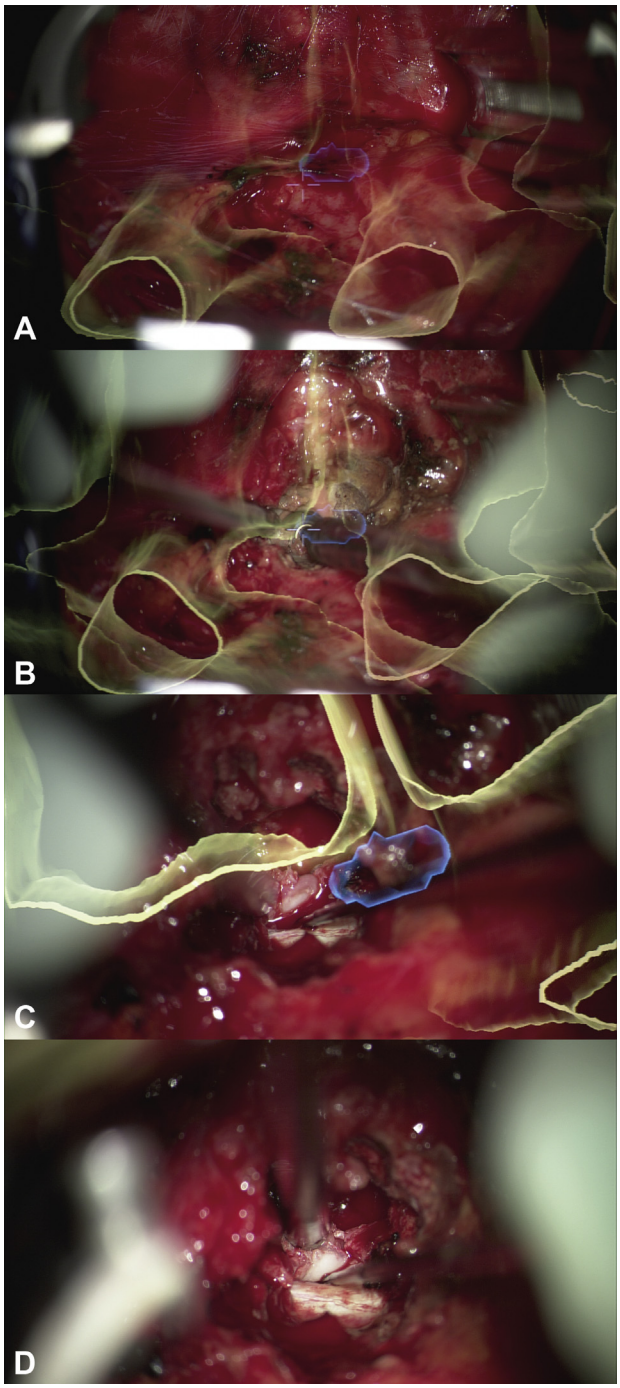

Figure 6. Augmented reality microscope view during the course of surgery (same patient as in Figure 5). In *yellow*, the 3-dimensional outlines of the vertebra and in *blue* the segmented disc herniation are visualized by the HUD. (**A**) After retractor placement, (**B**) bone drilling, (**C**) caudal mobilization of the disc fragment with a small hook, (**D**) microscope-view without AR while mobilizing the disc fragment.

data correspond well to our experience with iCT-based automatic registration in spine surgery. Besides its user independence, automatic iCT-based registration contributes to high AR accuracy because potential errors caused by positional shifting during the surgical approach and retractor placement can be excluded by scanning after performing the approach. Low-dose CT protocols ensured reduction of radiation exposure to a level of about 30% of standard spine CT scans. For procedures in the mid-thoracic region, relatively long scan ranges are required to ensure reliable nonlinear registration with the preoperative images. Further dose reduction might be possible, until a threshold is reached in which the lowered resolution and increased image noise prevent reliable nonlinear image registration.[22,23]

Radiation-free alternatives for registration are available; however, they do not provide the same accuracy as iCT-based registration. Surface matching techniques such as using a navigation pointer can only be used reliably for a single level and are not implemented for anterior, lateral, or paravertebral approaches. Attempts to use intraoperative ultrasound as an imaging alternative are still in its very infancy; the reported accuracy in phantom studies is not yet in the range that it can be applied for real surgery.[10,24]

To maintain AR accuracy during the course of surgery, several safety precautions have to be accounted for. As in cranial surgery, positional shifting causes inaccuracies because of a shifting of the coordinate system, so extraordinary diligence has to paid to exclude that there is a relative movement between surgical site and reference array. This is especially crucial in case the reference array is not attached to a spinous process and especially in lateral patient placement, where a tight fixation to the operating table is recommended. Additionally, to positional shifting the flexibility of the spine, being greatest in the cervical spine, poses additional challenges, as well as surgical maneuvers can also change the geometry of the spine by altering the inter-relation of vertebra bodies especially in regard to sagittal alignment. To reduce these influences, we performed registration scanning after placement of the retractor systems. Repeated landmark checks using the fiducials placed on the skin for calculating the registration error, as well as using clearly identifiable anatomical landmarks are advised. The navigation system issues a warning if the position of the reference array changes abruptly during surgery (e.g., an unwanted collision with an instrument), and immediate landmark checks are mandatory. In case of an increased inaccuracy, a repeated intraoperative registration scan applying low-dose iCT protocols is also advised, which also compensates for changes of the bony structures due to removal of them by a structure update.

In contrast to the early AR visualization for cranial surgery displaying dotted green outlines in the microscope HUD,[3-7] the current AR visualization provides an improved 3-D impression and depth visualization; however, it is not yet perfect, there is still potential for improvement. Besides improving the resolution of the AR display, an adjusted contrast or flexible color assignment has to be developed to ensure that different objects are equally visible, especially if some of them resemble in color the actual reality (e.g., a red object on a red background).

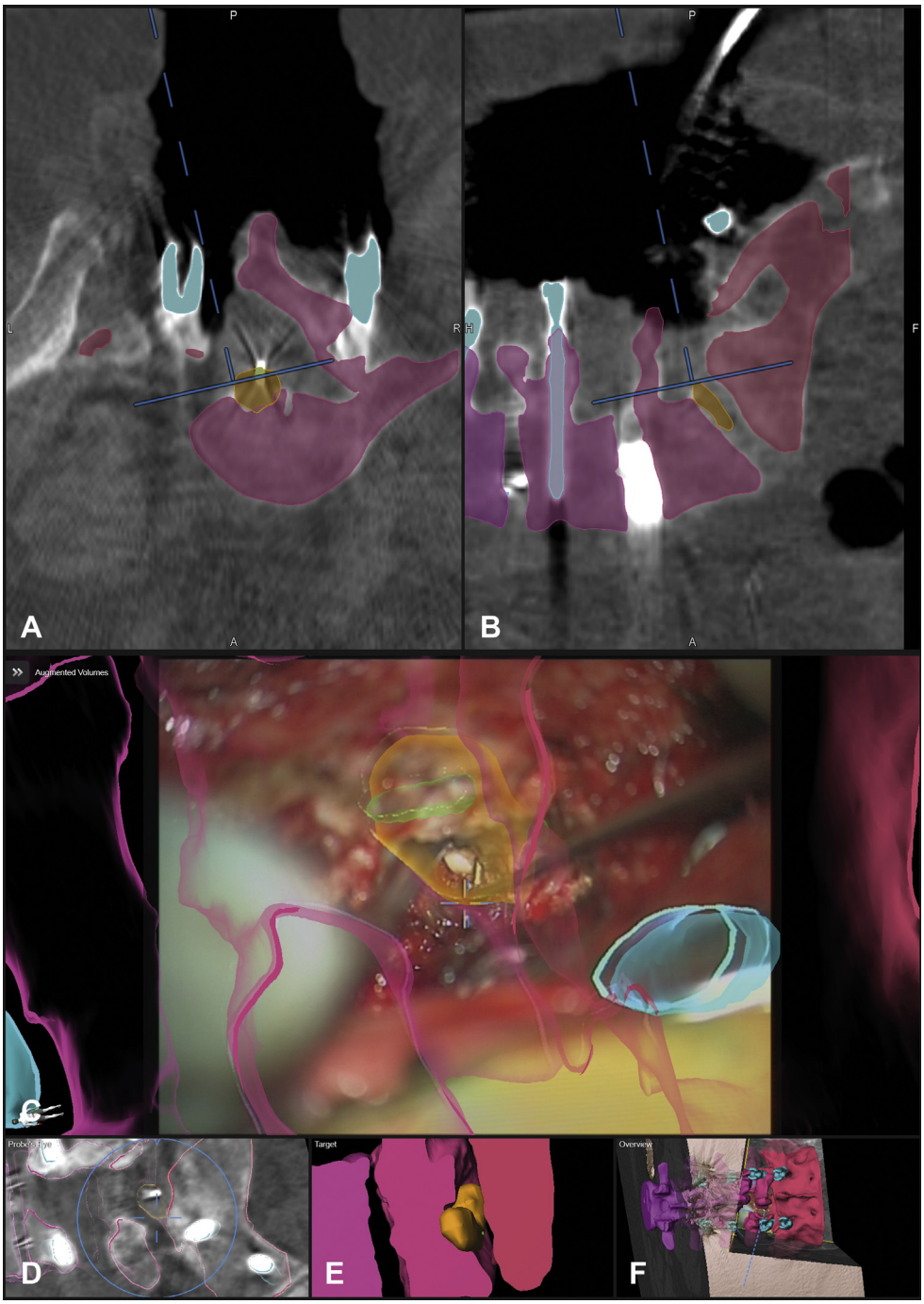

Figure 7. A 38-year-old female patient (case 4) with adjacent-level disease after spondylodesis and pseudarthrosis L5/S1 undergoing a cage revision and extension of the spondylodesis via a midline approach. (**A**) Axial and (**B**) sagittal views of navigation screen depicting the intraoperative computed tomography images with the segmented structures of the vertebra outlines (*pink*), the screws (*light blue*), the cage (*orange*), and the x-ray marker of the cage (*green*). (**C**) AR visualization depicting the close matching of the 3-dimensional cage object and the actual cage, which is partially visible and dissected with a small hook. (**D**) Probe's eye view, (**E**) target view; (**F**) overview visualization.

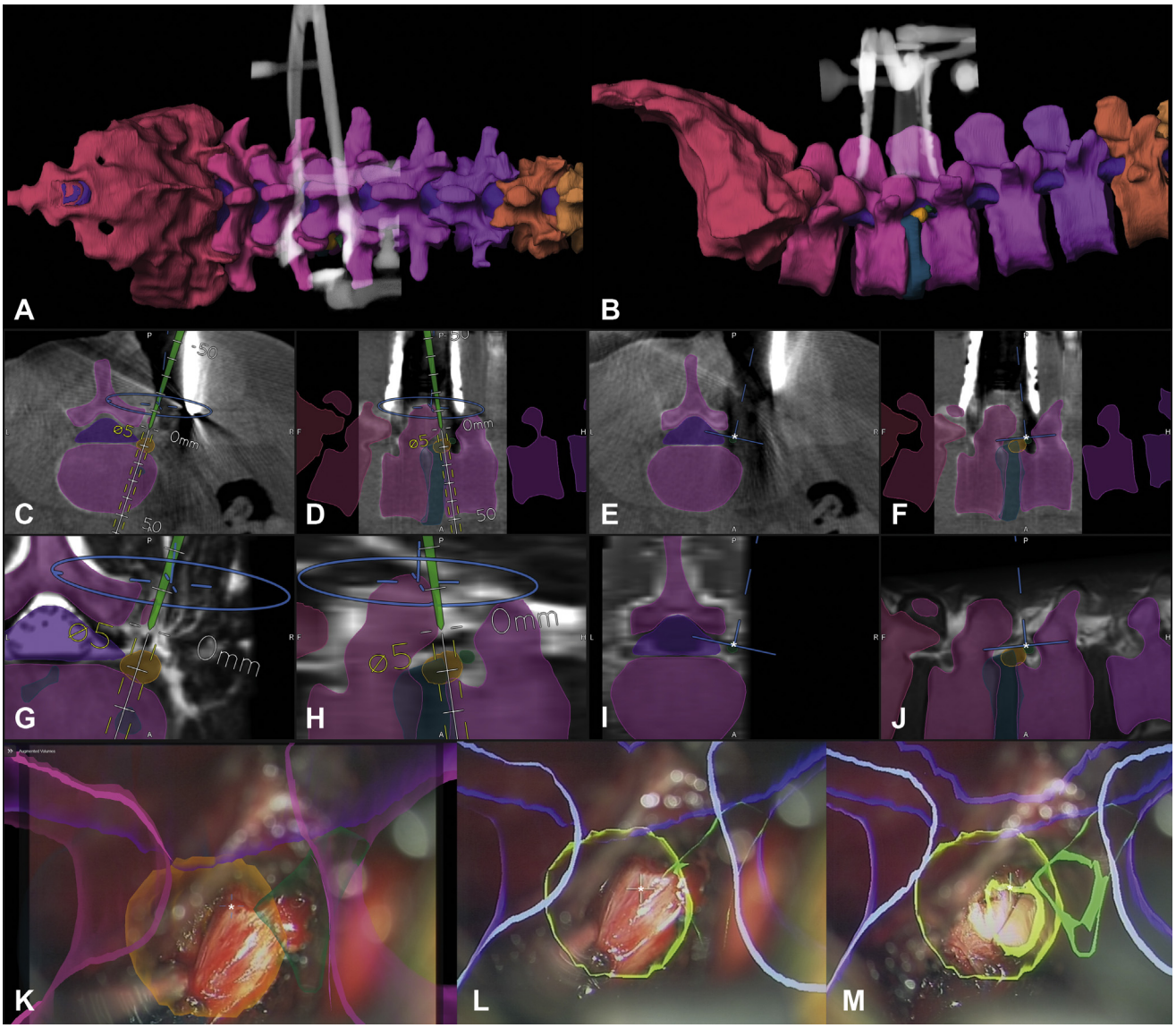

Figure 8. A 44-year-old male patient (case 5) with a right-sided lateral disc herniation at the level L3/L4, which is removed via a paramedian lumbar approach. (**A**) Posterior and (**B**) lateral views of a 3-dimensional rendering based on the intraoperative computed tomography (iCT) images depicting the position of the retractor, the vertebras are colored individually, the disc L3/L4 is segmented in *dark green*, the disc fragment in *yellow*, and the nerve root is colored *green*. (**C**) Axial and (**D**) sagittal view of iCT images, additionally to the operating microscope the navigation pointer is placed in the surgical field allowing to point at certain structures and offering the possibility for intraoperative distance measurements, corresponding to (**E**) axial; (**F**) sagittal view of iCT images; (**G**) axial and (**H**) sagittal views of T2-weighted magnetic resonance images with the navigation pointer in place; (**I**) axial and (**J**) sagittal views of T2-weighted magnetic resonance images without the navigation pointer. (**K**) Augmented reality visualization on screens; (**L**) augmented reality visualization applying the microscope head-up display, the nerve root is still covering the direct view of the disc fragment. (**M**) After mobilizing the nerve root, the disc fragment is visible (the crosshair in the center of panels **K**, **L**, and **M** corresponds to the microscope focus position in panels **E**, **F**, **I**, and **J**, all marked with an *asterisk*).

Additionally, AR has to be more immersive, not distracting the surgeon, and the digital content should not only be displayed on top of the real world image, but also the content should interact with the real world image, providing a merged reality.

Independent of its mode of implementation, AR has a huge potential for degenerative spine surgery. It may support surgery in complicated anatomical situations, like scars, reoperations, and anatomical variants, as well as facilitating surgery and shortening a learning period in standard procedures. Microsurgical procedures will tend to AR solutions based on operating microscopes, whereas percutaneous procedures such as kyphoplasty,[8,18] facet joint injections,[11] biopsies, and placement of pedicle screws[9,10,19]

probably will be candidates for head-mounted device—based AR.[25] Endoscopic AR might be the domain for even less minimal invasive procedures.

Additionally, AR has a huge potential as an educational tool by improving and facilitating the understanding of the complex 3-D spine anatomy. In a recent study on a mixture of physical and virtual simulation for spine surgery, it could be shown that the combination of these tools may potentially improve and abbreviate the learning curve for trainees, in a safe environment.[26] Such a system would also be a perfect choice to add mixed reality or AR support, which then would resemble the real intraoperative setting and support system.

The small sample size is a limitation of our study; however, we believe that we could prove the concept of microscope-based AR for degenerative spine surgery applying commercially available system components. Whether AR actually improves clinical outcome in degenerative spine surgery has to be investigated in further studies. Most likely, reoperations where anatomical landmarks are missing might benefit most from AR. Measurements of benefits of AR for resident education will need larger patient series.

CONCLUSIONS

Reliable microscope-based AR support is possible due to automatic registration based on intraoperative imaging. Application of AR in degenerative spine surgery has a big potential, it might be especially helpful in complex anatomical situations and resident education.

REFERENCES

1. Kelly PJ, Alker GJ Jr, Goerss S. Computer-assisted stereotactic microsurgery for the treatment of intracranial neoplasms. *Neurosurgery*. 1982;10:324-331.
2. Roberts DW, Strohbehn JW, Hatch JF, Murray W, Kettenberger H. A frameless stereotaxic integration of computerized tomographic imaging and the operating microscope. *J Neurosurg*. 1986;65:545-549.
3. Kiya N, Dureza C, Fukushima T, Maroon JC. Computer navigational microscope for minimally invasive neurosurgery. *Minimal Invas Neurosurg*. 1997;40:110-115.
4. King AP, Edwards PJ, Maurer CR, et al. A system for microscope-assisted guided interventions. *Stereo Funct Neurosurg*. 1999;72:107-111.
5. Fahlbusch R, Nimsky C, Ganslandt O, Steinmeier R, Buchfelder M, Huk W. The Erlangen concept of image guided surgery. In: Lemke HU, Vannier MW, Inamura K, Farman A, eds. *CAR'98*. Amsterdam: Elsevier Science B.V.; 1998:583-588.
6. Nimsky C, Ganslandt O, Kober H, et al. Integration of functional magnetic resonance imaging supported by magnetoencephalography in functional neuronavigation. *Neurosurgery*. 1999;44:1249-1255.
7. Nakamura M, Tamaki N, Tamura S, Yamashita H, Hara Y, Ehara K. Image-guided microsurgery with the Mehrkoordinaten Manipulator system for cerebral arteriovenous malformations. *J Clin Neurosci*. 2000;7(Suppl 1):10-13.
8. Abe Y, Sato S, Kato K, et al. A novel 3D guidance system using augmented reality for percutaneous vertebroplasty: technical note. *J Neurosurg Spine*. 2013;19:492-501.
9. Elmi-Terander A, Skulason H, Soderman M, et al. Surgical navigation technology based on augmented reality and integrated 3D intraoperative imaging: a spine cadaveric feasibility and accuracy study. *Spine (Phila Pa 1976)*. 2016;41:E1303-E1311.
10. Ma L, Zhao Z, Chen F, Zhang B, Fu L, Liao H. Augmented reality surgical navigation with ultrasound-assisted registration for pedicle screw placement: a pilot study. *Int J Comput Assist Radiol Surg*. 2017;12:2205-2215.
11. Agten CA, Dennler C, Rosskopf AB, Jaberg L, Pfirrmann CWA, Farshad M. Augmented reality-guided lumbar facet joint injections. *Invest Radiol*. 2018;53:495-498.
12. Kosterhon M, Gutenberg A, Kantelhardt SR, Archavlis E, Giese A. Navigation and image injection for control of bone removal and osteotomy planes in spine surgery. *Oper Neurosurg (Hagerstown)*. 2017;13:297-304.
13. Umebayashi D, Yamamoto Y, Nakajima Y, Fukaya N, Hara M. Augmented reality visualization-guided microscopic spine surgery: transvertebral anterior cervical foraminotomy and posterior foraminotomy. *J Am Acad Orthop Surg Glob Res Rev*. 2018;2:e008.
14. Carl B, Bopp M, Pojskic M, Voellger B, Nimsky C. Standard navigation versus intraoperative computed tomography navigation in upper cervical spine trauma. *Int J Comput Assist Radiol Surg*. 2019;14:169-182.
15. Carl B, Bopp M, Sass B, Nimsky C. Intraoperative computed tomography as reliable navigation registration device in 200 cranial procedures. *Acta Neurochir (Wien)*. 2018;160:1681-1689.
16. Huda W, Ogden KM, Khorasani MR. Converting dose-length product to effective dose at CT. *Radiology*. 2008;248:995-1003.
17. Elbakri IA, Kirkpatrick ID. Dose-length product to effective dose conversion factors for common computed tomography examinations based on Canadian clinical experience. *Can Assoc Radiol J*. 2013;64:15-17.
18. Deib G, Johnson A, Unberath M, et al. Image guided percutaneous spine procedures using an optical see-through head mounted display: proof of concept and rationale. *J Neurointerv Surg*. 2018;10:1187-1191.
19. Yoon JW, Chen RE, Han PK, Si P, Freeman WD, Pirris SM. Technical feasibility and safety of an intraoperative head-up display device during spine instrumentation. *Int J Med Robot*. 2017;13.
20. Meola A, Chang SD. Letter: Navigation-linked heads-up display in intracranial surgery: early experience. *Oper Neurosurg (Hagerstown)*. 2018;14:E71-E72.
21. Carl B, Bopp M, Voellger B, Sass B, Nimsky C. Augmented reality in transsphenoidal surgery [e-pub ahead of print]. *World Neurosurg* https://doi.org/10.1016/j.wneu.2019.01.202. Accessed February 11, 2019.
22. Greffier J, Pereira FR, Viala P, Macri F, Beregi JP, Larbi A. Interventional spine procedures under CT guidance: how to reduce patient radiation dose without compromising the successful outcome of the procedure? *Phys Med*. 2017;35:88-96.
23. Sarwahi V, Payares M, Wendolowski S, et al. Low-dose radiation 3D intraoperative imaging how low can we go? An O-arm, CT scan, cadaveric study. *Spine*. 2017;42:E1311-E1317.
24. Nagpal S, Abolmaesumi P, Rasoulian A, et al. A multi-vertebrae CT to US registration of the lumbar spine in clinical data. *Int J Comput Assist Radiol Surg*. 2015;10:1371-1381.
25. Yoon JW, Chen RE, Kim EJ, et al. Augmented reality for the surgeon: systematic review. *Int J Med Robot*. 2018;14:e1914.
26. Coelho G, Defino HLA. The role of mixed reality simulation for surgical training in spine: phase 1 validation. *Spine (Phila Pa 1976)*. 2018;43:1609-1616.

Conflict of interest statement: B. Carl and C. Nimsky received speaker fees from Brainlab.

Received 20 March 2019; accepted 22 April 2019

Citation: World Neurosurg. (2019) 128:e541-e551. https://doi.org/10.1016/j.wneu.2019.04.192

*Journal homepage: **www.journals.elsevier.com/world-neurosurgery***

*Available online: **www.sciencedirect.com***

1878-8750/$ - see front matter